Comparing and evaluating alternative methods to account for shallow site effects in hybrid broadband ground-motion simulations

Felipe Kuncar [i)], Brendon A. Bradley [i)], Christopher A. de la Torre [i)], Adrian Rodriguez-Marek [ii)], Chuanbin Zhu[i)], and Robin L. Lee [i)]

i) Department of Civil and Natural Resources Engineering, University of Canterbury, Christchurch, New Zealand.
ii) Department of Civil and Environmental Engineering, Virginia Tech, Blacksburg, United States.

ABSTRACT

Shallow site effects are usually not explicitly modelled in hybrid broadband ground-motion simulations, and their proper incorporation may be key to improving prediction at soil sites. This paper examines five methods to adjust hybrid simulations to account for these effects. These methods require different levels of site-characterization data: Methods 1 and 2 only use proxy parameters (e.g., V_{S30}, $Z_{1.0}$) to describe the site conditions, with Method 1 relying solely on proposed site adjustments in existing ground-motion models and Method 2 incorporating a host-to-target adjustment; Methods 3 and 4 use a shear-wave velocity profile along with two different frequency-domain approaches to predict the linear site response, coupled with the nonlinear component of Method 1; and Method 5 uses time-domain wave propagation analysis, and generally requires additional data to constrain nonlinear constitutive-model input parameters. Preliminary results of a validation study using 1000+ ground motions recorded at multiple strong-motion stations in the Canterbury Region (New Zealand) are provided. The results show that the incorporation of shallow site effects can significantly improve the accuracy of simulations. However, Method 1 tends to produce overamplification at relatively long vibration periods. An explanation for this phenomenon is provided in the paper and different strategies to mitigate this issue are discussed.

Keywords: local site effects, hybrid broadband ground-motion simulations, ground-motion prediction, validation

1 INTRODUCTION

Physics-based ground-motion simulations require the modelling of source, path, and site effects. Shallow site effects (i.e., those produced in the first ~100 m) are controlled by the near-surface sediments, but their inclusion in regional-scale simulations requires a finer spatial resolution in the material modelling than that typically considered. Thus, shallow site effects are usually not explicitly modelled. Two reasons hinder their explicit incorporation: (1) the high computational cost associated with a finer discretization of the domain and modelling of soil nonlinearity, and (2) the lack of detailed knowledge of the soil properties at the site of interest. Due to these limitations, shallow site effects are typically accounted for through a posterior adjustment to the simulated ground motions.

The results from some previous validation studies (e.g., de la Torre et al., 2020; Lee et al., 2022) suggest that the proper modelling of shallow site effects is key to improving ground-motion prediction at soil sites. This paper investigates five methods that can be adopted to adjust hybrid broadband ground-motion simulations to account for these effects. Also, preliminary results of a validation study are provided.

2 HYBRID BROADBAND GROUND-MOTION SIMULATIONS

2.1 Overview

This study focuses on ground-motion simulations performed with hybrid methods, which allow for the generation of realistic broadband ground-motion time series in the frequency range relevant to structural and geotechnical systems (Baker et al., 2021). These methods combine a comprehensive physics-based approach for the simulation of the low frequencies (LF) with a simplified physics-based approach for the simulation of the high frequencies (HF). In this study, the commonly used Graves and Pitarka (2010) hybrid simulation method is adopted, and the transition frequency between the LF and HF components is set to f=1 Hz.

2.2 Considerations for the modeling of site effects

Figure 1 shows the simulated shear-wave velocity (V_S) profiles used in hybrid broadband ground-motion simulations conducted by Lee et al. (2022) for a site located in Christchurch, New Zealand (strong-motion station PRPC). The LF simulated V_S profile was extracted at this location from the velocity model considered in the 3D numerical simulation performed for

the LF component ($f \leq 1$ Hz). This velocity model is based on the New Zealand Velocity Model (Thompson et al., 2020), but considers a minimum V_S of 500 m/s and a grid spacing of 100 m. The HF simulated Vs profile corresponds to a generic 1D profile considered for the whole country in the semi-stochastic approach used for simulating the HF component ($f > 1$ Hz). Figure 1 also shows the site-specific V_S profile measured at this location using surface-wave testing.

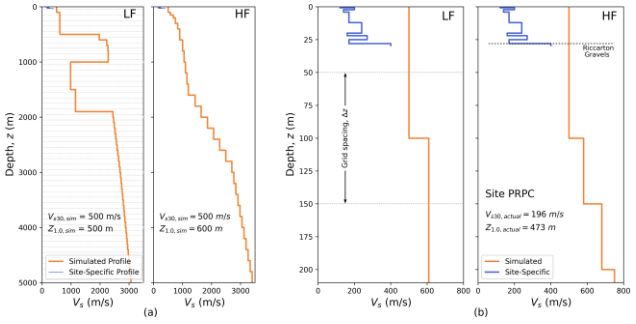

Fig. 1. LF and HF simulated and site-specific (measured) Vs profiles at the site PRPC, located in Christchurch, New Zealand. (a) 5000 m deep. (b) 210 m deep.

Figure 1 illustrates some common features of hybrid broadband ground-motion simulations that must be accounted for when adjusting them to incorporate shallow site effects:

1. The two approaches (LF and HF) can consider different velocity structures. This means that different adjustments may need to be considered for each component.

2. The minimum V_S considered is usually too high (e.g., 500 m/s in this case) and the spatial resolution is typically too coarse (e.g., 100-m grid spacing in the LF simulation considered here) to capture shallow site effects.

3. Local site effects can be captured to some extent. (e.g, deep basin effects can be captured by the 3D simulation performed for the LF component). Thus, the adjustment should not double-count these effects.

4. Although not illustrated in Figure 1, soil nonlinearity is usually not modelled in the regional ground motion simulations (as is the case in this study), and therefore the adjustment must incorporate it.

3 SHALLOW-SITE-EFFECT ADJUSTMENT

3.1 Frequency-domain and time-domain adjustments

The adjustment to account for shallow site effects can be performed in the frequency domain or in the time domain. In the first approach, a site factor (SF) is applied to the simulated ground motion in the frequency (Fourier) domain, and then the adjusted ground motion is converted back to the time domain. The second approach involves performing 1D, 2D, or 3D time-domain nonlinear inelastic site-response analysis. Both procedures produce a waveform that includes the influence of shallow site effects, but in the case of the second approach, soil nonlinearity is explicitly modeled in the time domain.

Four methods (Methods 1 to 4) to develop the site factor in the frequency-domain approach are investigated, in addition to an implementation of the time-domain adjustment based on 1D nonlinear inelastic site-response analysis (Method 5).

3.2 Methods considered

Table 1 summarizes the five methods investigated. These methods represent a wide range of options that can be used when different levels of site-characterization data are available. Methods 1 and 2 only require simple site parameters to describe the site conditions, which makes them more suitable for regional applications. Methods 3 and 4 can be applied when a V_S profile is available, and Method 5 represents a more sophisticated approach that generally requires further site-characterization data.

Table 1. Methods considered to adjust simulated ground motions to account for unmodelled shallow site effects.

Method	Description	Required data
1	Frequency-domain adjustment based on the site-response component of GMMs	V_{S30} (and $Z_{1.0}$)
2	Similar to Method 1 but includes a host-to-target adjustment	V_{S30} (and $Z_{1.0}$)
3	Frequency-domain adjustment that combines the SRI method with the nonlinear component of Method 1	V_S and ρ profiles, and κ_0
4	Frequency-domain adjustment that combines the theoretical 1D transfer function with the nonlinear component of Method 1	V_S, ρ, and D_{min} profiles
5	Time-domain adjustment based on 1D nonlinear inelastic wave-propagation analysis	V_S and ρ profiles, D_{min}, and constitutive model parameters

Method 1 uses the site-response component (f_S) of one of the existing semi-empirical ground-motion models (GMMs) for Fourier amplitude spectra (FAS), or alternatively, for pseudo-spectral acceleration (SA). This corresponds to the standard approach originally proposed by Graves and Pitarka (2010) to account for shallow site effects. The site factor derived by Method 1 (SF_1) can be generally expressed as

$$SF_1 = \frac{\exp[f_S(f, V_{S30,actual}, IM_{rock})]}{\exp[f_S(f, V_{S30,sim})]} = SF_{1,L} \cdot SF_{1,NL} \quad (1)$$

where $V_{S30,actual}$ and $V_{S30,sim}$ are the 30-m time-average shear-wave velocity measured (or estimated) at the site and considered in the regional ground-motion simulation, respectively. In the case of the site PRPC (Figure 1), $V_{S30,actual}$=196 m/s, and $V_{S30,sim}$=500 m/s for both the LF and HF components. IM_{rock} corresponds to an intensity measure (IM) computed at a reference condition (stiff soil or rock) and it is used to

define the magnitude of the soil nonlinearity. If the f_{sed} term (scaling with sediment thickness, usually defined in GMMs) is included in f_S, an additional parameter representative of the depth of the sediments (e.g., $Z_{1.0}$, which is defined as the depth from the surface to the V_S horizon of at least 1 km/s) is required for the actual and simulated conditions. $SF_{1,L}$ and $SF_{1,NL}$ represent the linear and nonlinear components of SF_1, respectively.

Some previous validation studies (e.g., de la Torre et al., 2020; Lee et al., 2022) have found that Method 1 tends to produce systematic overamplification at relatively long vibration periods (relatively low frequencies). This can be partially explained by the inconsistency between the situation to be modelled and that implicit in the host V_S profiles of the selected GMM (Figure 2). Figure 2(a) assumes that the deep velocity structure of the actual site condition (actual profile) is properly modelled by the regional ground-motion simulation (simulated profile), but an adjustment is required to incorporate the site effects generated by the actual near-surface soil layers, characterized by lower velocities than the $V_{S,min}$ considered in the regional simulation. As illustrated in Figure 2(a), the host profiles implicit in the GMM for $V_{S30,actual}$ and $V_{S30,sim}$ will generally display significant differences at depth, due to the positive correlation that usually exists between V_{S30} and V_S at depth in a typical geological environment (Kamai et al., 2016). This difference (which does not exist between the actual and simulated profiles) translates into overamplification at relatively low frequencies.

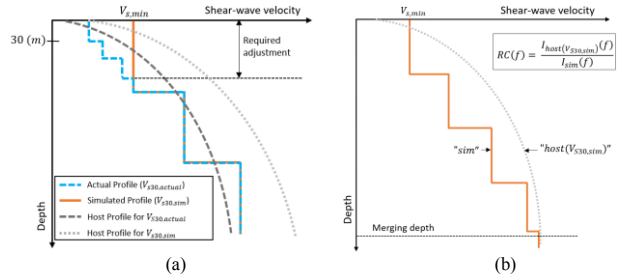

Fig. 2. Illustration of (a) the host-to-target conversion issue present in Method 1, and (b) the computation of the reference correction factor introduced in Method 2.

Al Atik and Abrahamson (2021) developed a method to estimate the 1D host V_S profiles implicit in a GMM. They also showed that the derivation of these 1D host profiles is only appropriate in the case of relatively stiff site conditions, which are less influenced by 2D/3D effects. Using the reference host profile obtained by this approach, a method is proposed here to adjust the Method 1 site factor (SF_1). This method, referred to as Method 2, is inspired by the approach proposed by Williams and Abrahamson (2021). The site factor in Method 2 (SF_2) can be expressed as follows:

$$SF_2 = SF_1 \cdot \frac{I_{host(V_{S30,sim})}}{I_{sim}} = SF_1 \cdot RC \qquad (2)$$

where $I_{host(V_{S30,sim})}$ and I_{sim} are the impedance-based site amplifications produced by the host profile for $V_{S30,sim}$ and by the simulated profile, respectively, and RC is the reference correction factor. These profiles are illustrated in Figure 2(b). The impedance-based amplifications are computed using the Square-Root Impedance (SRI) method (Boore, 2013), relative to a common elastic half-space, located at or below the merging depth indicated in Figure 2(b). This host-to-target adjustment intends to ensure consistency with the reference condition implicit in the GMM for $V_{S30,sim}$, but does not address the potential inconsistency with the site conditions implicit in the GMM for $V_{S30,actual}$, which is a common limitation of any method based on V_{S30} (i.e., ergodic approach).

Method 3 requires a V_S profile and uses the SRI method and the nonlinear operator from Method 1 (based on V_{S30}). The site factor (SF_3) can be expressed as

$$SF_3 = \frac{TF_{SRI,actual}}{TF_{SRI,sim}} \cdot SF_{1,NL} \qquad (3)$$

where $TF_{SRI,actual}$ and $TF_{SRI,sim}$ are the transfer functions computed for the actual and simulated profile, respectively, relative to a common half-space. As illustrated in Figure 3, this requires the connection of the two profiles at a given depth. If the site-specific V_S profile available is not deep enough, complementary sources of information can be used to extend it. In this case, the NZVM is used. As shown in Figure 3, the computation must be performed separately for the LF and HF components, given that the simulated profile may be different (in this particular case, the velocity at the half-space is only slightly different).

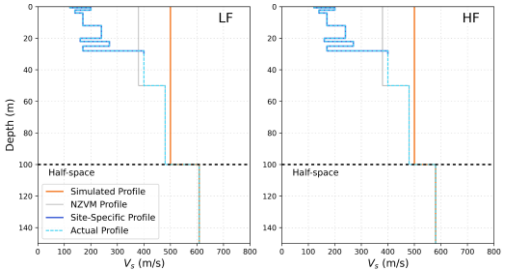

Fig. 3. Profiles considered in Methods 3 and 4 for the site PRPC.

The goal of $TF_{SRI,sim}$ is to remove the near-surface site effects introduced by the simulation, to then account for them in a site-specific fashion through $TF_{SRI,actual}$. Since the HF site response in the Graves and Pitarka methodology is modeled through the SRI method, this method is also used in the denominator of eq. (3), for consistency. In this manner, SF_3 can be expressed as

$$SF_3 = \sqrt{\frac{\bar{\rho}_{sim}\bar{V}_{S,sim}}{\bar{\rho}_{actual}\bar{V}_{S,actual}}} \cdot \exp\left[-\pi f\left(\kappa_{0,actual} - \kappa_{0,sim}\right)\right] \cdot SF_{1,NL} \quad (4)$$

where $\bar{\rho}_{sim}$ and $\bar{V}_{S,sim}$ are the travel-time weighted average density and V_S of the simulated profile, respectively, from the surface to a depth equivalent to a quarter-wavelength of each frequency considered; $\bar{\rho}_{actual}$ and $\bar{V}_{S,actual}$ are the corresponding values for the actual profile; and $\kappa_{0,actual}$ and $\kappa_{0,sim}$ are the actual and simulated high-frequency site attenuation parameters. In the case of the regional ground motion simulations used in this study, a constant value of $\kappa_{0,sim}$=0.045 s was considered for the entire country (Lee et al., 2022). In this paper, $\kappa_{0,actual}$ is estimated through a correlation with V_{S30} (Bayless and Abrahamson, 2019).

Method 4 is similar to Method 3, but uses the theoretical 1D transfer function instead of the SRI method to model the linear site response:

$$SF_4 = \frac{TF_{1D}(V_{S,actual}, \rho_{actual}, D_{min,actual}, V_R, \rho_R, D_{min,R})}{\sqrt{\frac{\rho_R V_R}{\bar{\rho}_{sim}\bar{V}_{S,sim}}} \cdot \exp\left[-\pi f \Delta\kappa_{0,sim}\right]} \cdot SF_{1,NL} \quad (5)$$

where $V_{S,actual}$, ρ_{actual}, and $D_{min,actual}$ are the V_S, density, and small-strain damping of the actual profile; V_R, ρ_R, $D_{min,R}$, are corresponding values for the elastic half-space; and $\Delta\kappa_{0,sim}$ is the difference between $\kappa_{0,sim}$ (measured from the surface) and κ_0 measured from the elastic half-space. Unlike $\kappa_{0,sim}$, $\Delta\kappa_{0,sim}$ is not a direct input parameter of the HF simulation, and hence, it must be estimated. Here, $D_{min,actual}$ and $\Delta\kappa_{0,sim}$ are estimated through a correlation with V_S (Campbell, 2009).

Method 5 involves the deconvolution of the ground motion down to a proper reference condition, and the subsequent 1D time-domain nonlinear inelastic site-response analysis to capture the actual site conditions (Figure 4). In the case of the site PRPC, the reference condition is selected at the start of the Riccarton Gravels (see Figure 1), which represents a stiff soil condition where nonlinear effects are considered negligible. In this study, the site-response analyses are conducted in OpenSees (McKenna, 2011) using the plasticity-based constitutive models PDMY02 and PIMY (Yang et al., 2003). The determination of the model parameters (e.g., friction angle, cohesion) involved the use of CPT data available at the site.

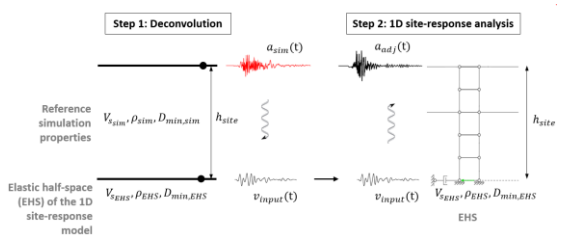

Fig. 4. Illustration of Method 5.

3.3 Comparison between methods

Figure 5 presents a comparison of the five Methods for the site PRPC and two earthquakes. These events produced a low- and a high-amplitude ground motion, which allows for illustrating a case where the soil behaves almost in the linear range, and a case where significant soil nonlinearity is produced. The top panels [Fig. 5(a) and 5(b)] present the site factors (developed through Methods 1 to 4) and the bottom panels [Fig. 5(c) and 5(d)] display the resulting amplification factors (AFs) for SA (i.e., the ratio between the adjusted and unadjusted SA), including those obtained by Method 5. In the case of Methods 1, 3 and 4, two different GMMs are considered: CB14 (Campbell and Bozorgnia, 2014) and BA18 (Bayless and Abrahamson, 2019). The former was developed in the response spectral domain and the latter in the Fourier spectral domain. Method 2 only considers the CB14 model.

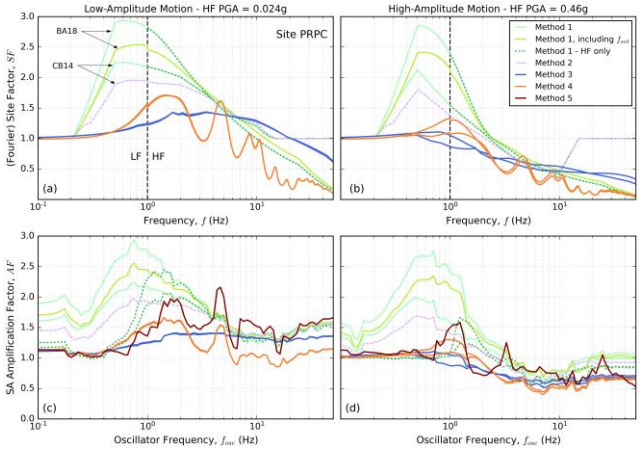

Fig. 5. Comparison of methods in terms of site factors (SFs) and the resulting response spectral amplification factors (AFs). SFs for (a) the low-amplitude and (b) high-amplitude motions. Response spectral AFs for (c) the low-amplitude and (d) high-amplitude motions.

Figure 5 shows a significant variability between methods. Method 1 produces considerable amplification at low frequencies relative to the other methods, even though a low-frequency truncation was applied, such as in de la Torre et al. (2020). This is consistent with the findings of some previous validation studies. Figure 5 illustrates different strategies to reduce this overamplification: (1) including the term f_{sed}; (2) applying SF_1 to the HF simulation component only, such as in Lee et al. (2022); (3) using Method 2; and (4) selecting a GMM that minimizes this issue (in this case the CB14 model displays considerably less overamplification than the BA18 model).

Figure 5 also illustrates the differences between an ergodic treatment of soil nonlinearity based on V_{S30} (Methods 1 to 4) and a site-specific treatment of it as in Method 5. The latter is able to capture site-specific features such as the softening of the resonance peaks in the response spectral amplification, whereas the ergodic

approach simply results in a general reduction and smoothing of the linear amplification.

4 VALIDATION STUDY

4.1 Overview

Since all the methods are based on certain simplifications and assumptions (e.g., Method 5 relies on the 1D assumption) it is not possible to stablish the best method *a priori*. To investigate the relative performance of each method under different site conditions, a systematic comparison with observed ground motions is needed. This section presents preliminary results from a validation study being conducted in New Zealand using multiple strong-motion stations across the country. The results discussed here correspond to the Canterbury Region only.

4.2 Sites and earthquakes considered

Figure 6 shows the 20 strong-motion-station sites and 158 earthquakes considered.

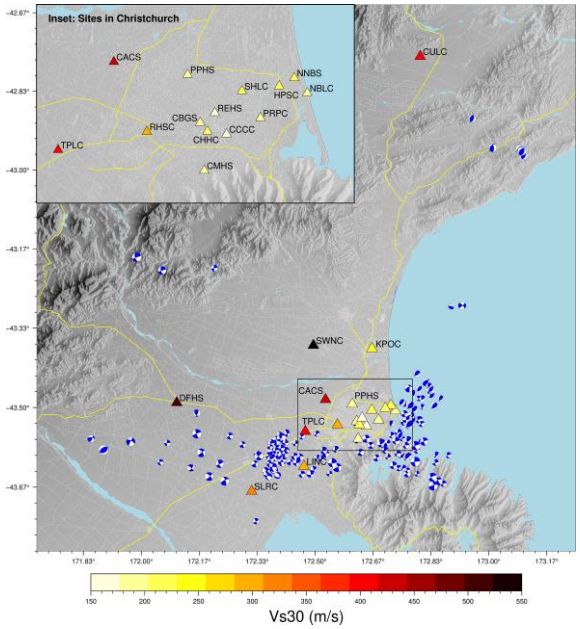

Fig. 6. Location of the 20 sites and 158 earthquake sources considered in this study (Canterbury Region, New Zealand).

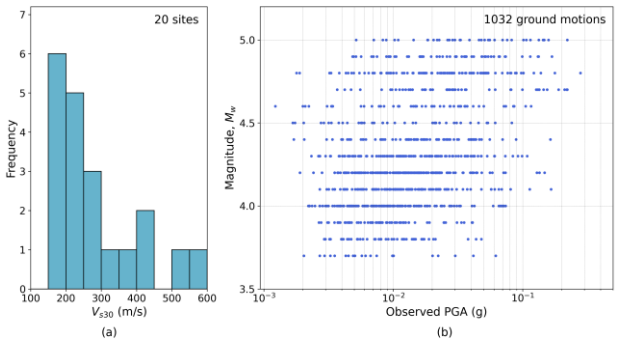

Fig. 7. (a) V_{S30} distribution of the 20 sites. (b) Magnitude-PGA distribution of the 1032 observed ground motions.

Site investigations have been conducted at each site (e.g., Wotherspoon, 2015), and as a result, at least one V_S profile derived from surface-wave testing is available at each location and CPT data are available at most of them. As illustrated in Figure 6 and Figure 7(a), these sites represent a wide range of soil conditions, including a considerable number of sites with V_{S30}≤300 m/s. The earthquakes considered are small-magnitude events (3.5≤M_w≤5.0) and their simulations were performed by Lee et al. (2022) using the Graves and Pitarka (2010) method. Despite the small magnitude of these events, Figure 7(b) shows that significant accelerations (PGA ≥ 0.1g) were observed at some stations. Considering the presence of relatively soft sites, this means that moderate levels of nonlinearity are expected at some locations. After imposing a minimum of 3 recordings per event and per station, the total number of observed ground motions considered is 1032.

4.3 Model bias and total variability

Methods 1, 3, 4, and 5 were applied to each simulated ground motion. Then, the prediction residual (Δ_{es}) for the spectral acceleration (SA) was computed using the following expression:

$$\Delta_{es} = \ln(SA_{obs})_{es} - \ln(SA_{sim})_{es} \quad (6)$$

where $\ln(SA_{obs})_{es}$ is the natural logarithm of the observed SA for the earthquake e and site s, and $\ln(SA_{sim})_{es}$ is the natural logarithm of the corresponding simulated SA.

Using mixed-effects regression the residuals were partitioned into different components of ground-motion variability:

$$\Delta_{es} = a + \delta S2S_s + \delta B_e + \delta W_{es}^0 \quad (7)$$

where a is the model bias, $\delta S2S_s$ is the site-to-site residual, δB_e is the between-event residual, and δW_{es}^0 is the remaining within event residual.

Figure 8(a) presents the resulting model bias (a) and Figure 8(b) the total standard deviation (σ) of the residuals for the different methods considered. The results for the original simulation (without shallow-site-effect adjustment) are also provided.

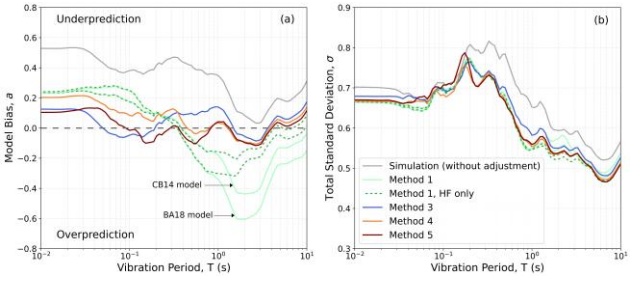

Fig. 8. Preliminary results of the ongoing validation study. (a) Model bias and (b) total standard for the 1032 ground motions considered for the different methods. For methods 3 and 4 only the CB14 model was considered.

Figure 8(a) shows that, on average, (1) the regional simulation without adjustment underpredicts SA over the entire period range; (2) the application of Method 1 results in a reduction of the underprediction at short vibration periods ($T \leq 0.3$s) but produces significant overprediction at longer periods; (3) the application of Method 1 to the HF range only, reduces this overamplification, but does not remove it; (4) the more site-specific methods (Methods 3 to 5) display the best performance, considerably reducing the model bias of the simulations in practically the entire period range. Figure 8(b) illustrates that the adjustment for shallow site effects using any of the investigated methods generally reduces the total standard deviation in the residuals relative to the unadjusted simulation, however, the differences between methods are not significant.

5 CONCLUSIONS

This study addressed the incorporation of shallow site effects in hybrid broadband ground-motion simulations. Five methods to adjust simulated ground motions to account for these effects were discussed, and preliminary results of an ongoing validation study were presented. The methods studied represent a wide range of options that require different levels of site-characterization data and expertise.

As shown in this paper and in previous validation studies, the most common approach to incorporate shallow site effects (Method 1, based on V_{S30}) can produce significant overamplification at relatively long vibration periods. Here, an explanation for this phenomenon was provided and alternative strategies to mitigate this issue were discussed, including a method involving a host-to-target correction (Method 2). In addition, two simple methods that can be applied if a V_S profile is available (Methods 3 and 4) were proposed and compared with a more advanced approach based on 1D time-domain nonlinear inelastic site-response analysis (Method 5).

The validation study showed that the incorporation of shallow site effects can significantly improve the accuracy of the ground-motion simulations and moderately improve their precision. On average, the more site-specific methods (Methods 3 to 5) displayed a better performance than the standard V_{S30} -based approach (Method 1). Methods 3 and 4 showed comparable performance to the more advanced Method 5, but the small-magnitude events considered in this study imply only limited levels of soil nonlinearity. The inclusion of additional sites and larger magnitude events in the validation study, as well as the more thorough analysis of the residuals (e.g., disaggregated by site), will provide additional insights into the relative performance of the different methods under different conditions.

ACKNOWLEDGMENTS

This work was financially supported by the Resilience to Nature's Challenges and Toka Tū Ake EQC.

REFERENCES

1) Al Atik, L. and Abrahamson, N. (2021): A methodology for the development of 1D reference V_S profiles compatible with ground-motion prediction equations: application to NGA-West2 GMPEs, *Bulletin of the Seismological Society of America*, 111(4), 1765-1783.
2) Baker, J., Bradley, B. and Stafford, P. (2021): Seismic hazard and risk analysis, *Cambridge University Press*.
3) Bayless, J. and Abrahamson, N. (2019): Summary of the BA18 ground-motion model for Fourier amplitude spectra for crustal earthquakes in California, *Bulletin of the Seismological Society of America*, 109(5), 2088-2105.
4) Bore, D. (2013): The uses and limitations of the square-root-impedance method for computing site amplification, *Bulletin of the Seismological Society of America*, 103(4), 2356-2368.
5) Campbell, K. (2009): Estimates of shear-wave Q and κ_0 for unconsolidated and semiconsolidated sediments in Eastern North America, *Bulletin of the Seismological Society of Americas*, 99(4), 2365-2392.
6) Campbell, K. and Bozorgnia, Y. (2014): NGA-West2 ground motion model for the average horizontal components of PGA, PGV, and 5% damped linear acceleration response spectra, *Earthquake Spectra*, 30(3), 1087-1115.
7) de la Torre, C., Bradley B. and Lee R. (2020): Modeling nonlinear site effects in physics-based ground motion simulations of the 2010-2011 Canterbury earthquake sequence, *Earthquake Spectra*, 36(2), 856-879.
8) Graves, R. and Pitarka, A. (2010): Broadband ground-motion simulation using a hybrid approach, *Bulleting of the Seismological Society of America*, 100(5A), 2095-2123.
9) Kamai, R., Abrahamson, N. and Silva, W. (2016): V_{S30} in the NGA GMPEs: Regional differences and suggested practice, *Earthquake Spectra*, 32(4), 2083-2108.
10) Lee, R., Bradley B., Stafford, P., Graves, R. and Rodriguez-Marek, A. (2022): Hybrid broadband ground-motion simulation validation of small magnitude active shallow crustal earthquakes in New Zealand, *Earthquake Spectra*, 38(4), 2548-2579.
11) McKenna, F. (2011): OpenSees: A framework for earthquake engineering simulation, *Computing in Science and Engineering*, 13(4), 58-66.
12) Thomson, E., Bradley, B. and Lee, R. (2020): Methodology and computational implementation of a New Zealand Velocity Model (NZVM2.0) for broadband ground motion simulation, *New Zealand Journal of Geology and Geophysics*, 63(1), 110-127.
13) Williams, T. and Abrahamson, N. (2021): Site-response analysis using the shear-wave velocity profile correction approach, *Bulletin of the Seismological Society of America*, 111(4), 1989-2004.
14) Wotherspoon, L., Orense, R., Bradley, B., Cox, B., Wood, C. and Green, R. (2015): Geotechnical characterization of Christchurch strong motion stations, *Earthquake Commission Report Project N. 12/629, Version 3*.
15) Yang, Z., Elgamal, A. and Parra, E. (2003): Computational model for cyclic mobility and associated shear deformation, *Journal of Geotechnical and Geoenvironmental Engineering*, 129(12), 1119-1127.